Optical Microscopy Beyond the Diffraction Limit

Niko F. van Hulst & Frans B. Segerink, Opto-electronics, Applied Physics, Univ. of Twente, The Netherlands

Keywords: Scanning Probe Microscopy; Scanning Near field Optical Microscopy; Evanescent field

Introduction

The art of microscopy is the result of centuries of development and yet the state of the art has passed a remarkable decade of innovation with the advent of scanning probe microscopy. The invention of the Scanning Tunneling Microscope (STM) only ten years ago by Binnig & Rohrer has rapidly spread into material science and the semiconductor industry for the inspection of thin films, crystal growth, defects, etc. down to the atomic level. The scanning probe technique is increasingly moving towards chemical and biological surfaces since it has been reinforced by atomic force microscopy (AFM) which is ideally suited for non-conductive surfaces and operation in fluids. Simultaneously image processing has become an indispensible aid for metrology, contrast enhancement, spatial frequency filtering, operations between images, sectioning, volume rendering, etc.

In optical microscopy laser scanning has become a routine technique, allowing 3D imaging, phase contrast, auto focus, fluorescence detection, etc. at a resolution approaching the ultimate diffraction limit in the confocal microscope (CFM). A primary disadvantage of conventional imaging optical microscopy is the lateral resolution which is limited by diffraction to dimensions of the wavelength because the detection is based on propagating homogeneous waves. Yet a light wave incident onto a sample is diffracted into both homogeneous and inhomogeneous waves. The inhomogeneous wave, which contains sub-wavelength information of the sample, is confined to the near field because it cannot propagate, it evanesces, and can only be detected by a probe in the near field at sub-wavelength distance from the sample.

The concept of near field microscopy as a means of observing structural details smaller than the wavelength of the field itself was pointed out long before STM; however due to practical limitations the use of evanescent waves was not considered as of practical importance to microscopy. The development of scanning probe microscopy has stimulated a fresh approach towards the practical exploitation of the optical near field in microscopy as it provides the technology to scan a highly localised probe which senses the interaction with a sample surface on a nanometre scale. A major advantage of Scanning Near Field Optical Microscopy (SNOM), compared to STM and AFM, is the fact that the interaction is optical, i.e. the electromagnetic field with its specific vectorial character and frequency; consequently the images contain polarisation contrast and spectroscopic information. All techniques of conventional optical microscopy can be adapted to SNOM provided the signal level is sufficient, e.g. detection of luminescence and polarisation effects

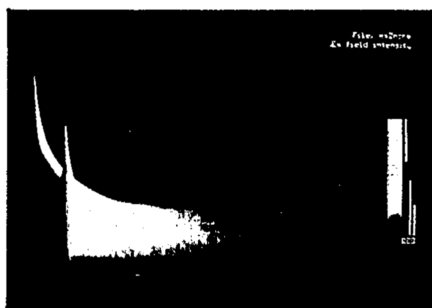

Fig. 1: Calculation of the near field intensity extending beyond an aperture (diameter $\phi \ll \lambda$) in a conducting screen. The intensity of the field component parallel to the incident polarisation direction is plotted over an area of $2\phi \times 2\phi$. The intensity peaks on the edges of the aperture in the polarisation direction.

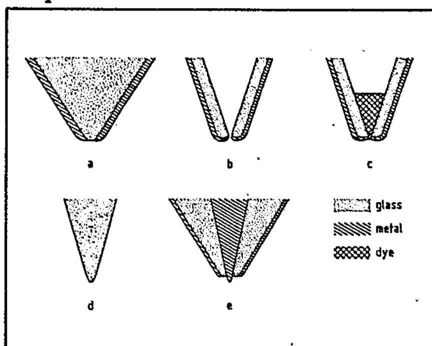

Fig. 2: Schematic outline of near field optical probe types:
(a) sub-micron aperture formed by a sharpened fibre (2) or glass tip (3) coated with metal.
(b) sub-micron aperture formed by a micro-pipette coated with metal (4).
(c) miniature fluorescent source formed by a dye matrix in a micro-pipette (5).
(d) sharpened optical fibre suitable as a leaky wave detector (6,7,8).
(e) miniature optical coaxial line (11).

and use of phase information, with a resolution approaching that of a SEM. This is a major improvement for optical spectroscopic applications. The microscope operates on dielectric surfaces in contrast to electron microscopy (SEM, STM) which is restricted to information associated with electrons and operates generally only on conductive surfaces under vacuum conditions.

In this paper the concept of near field optical imaging is discussed, different types of microscopes are reviewed and the capacity of SNOM is illustrated with recent advances of our evanescent field optical microscope.

Concept of near field imaging

In contrast to conventional optical microscopy SNOM is free of imaging optics. The optical electromagnetic field merely serves as a driving field with a wavelength appreciably larger than the imaging system. The heart of a near field optical microscope is a nanometre-size structure which serves as an optical antenna. An incident light beam diffracted at this structure is strongly divergent with a field strongly confined to its surface. The decay length is approximately equal to the dimensions of the micro-structure. The size of the antenna is appreciably smaller than the optical wavelength, as a result the spatial frequency spectrum of the field is dominated by correspondingly large wave numbers. This is the near field regime with its non-radiative evanescent waves. Spatial frequencies with small wave number are also present in the diffracted field and represent the weak far field radiation.

The distribution of the diffracted field is strongly sensitive to changes in the dielectric properties of the immediate surroundings of the antenna. A sample brought into the near field regime modifies the field distribution and alternatively the dielectric properties of the sample can be examined with a resolution corresponding to the antenna size (1).

The near field concept is illustrated in fig. 1 where the optical antenna is formed by an aperture in a thin metal film. A linearly polarised light beam with wavelength λ is incident on the aperture with diameter $\phi \ll \lambda$. The calculated field intensity beyond the aperture in the plane parallel to the incident polarisation direction is plotted in Fig. 1 over a square area of two aperture diameters, where the aperture is located at the left side and the wave propagates to the right. The field intensity within the hole is proportional to the area of the aperture. Due to boundary conditions the field intensity is enhanced on the edges of the aperture in directions associated with the polarisation of the incident field. Moving away from the aperture through the near field regime the non-radiative evanescent waves are damped out and the field intensity decreases strongly with a fourth power dependence on the distance. The influence of a dielectric sample on the field distribution decreases strongly in this regime. The field remains collimated to a distance of about the aperture size. At larger distance the radiation diverges strongly and the width of the profile increases linearly with the distance. At a distance of about the wavelength (far out of Fig. 1) the relation with the aperture size is completely lost, because the source dimension seems to be in the order of the wavelength itself. This is the transition to the far field regime where the field intensity decreases quadratically with the distance corresponding to a constant flux per steradian. The fraction of the field energy in the hole that radiates into the far field is only a tiny fraction of the incident flux while the majority

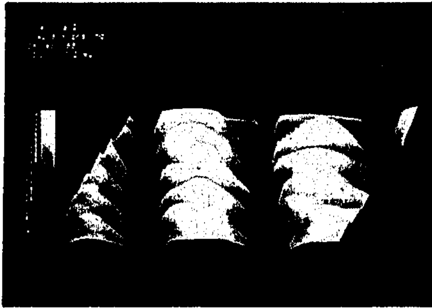

Fig. 3: 3×3 μm scan over a 1μm period SiN grating, with steps 500 nm wide and 350 nm high, in closed loop, with an s-polarised laser beam, with (upper) an average tip and (lower) a sharp tip with small apex angle.

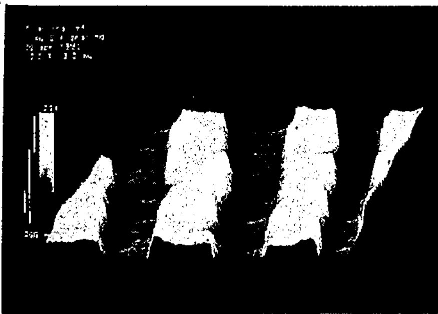

Fig. 4: 18.8×18.8 μm closed loop image of ϕ 951 nm latex spheres with laser beam incident from left to right.

Fig. 5: 11.2×11.2 μm image of a ϕ 91 nm latex sphere with laser beam incident from right to left scanned at constant height.

of the energy flows back and forth through the aperture.

Clearly to obtain maximum resolution and efficiency the distance between sample surface and optical antenna should be smaller than the antenna size. The near field distribution depends strongly on polarisation which implies polarisation contrast in imaging. Moreover the detected far field flux depends strongly on the antenna size, which again enhances contrast.

Probe types

The resolution of near field microscopy is mainly limited by the capability of fabricating nanometre size structures and the ability to detect the scattered far field. It is essentially impossible to illuminate a nanometre size structure efficiently because an optical focus is limited to wavelength dimensions. Moreover the far field of the diffracted light is detected which is only a small fraction of the driving field. Therefore resolution is gained at the expense of signal intensity. The problem of combining high resolution, high efficiency and reliability has stimulated the development of several types of near field probe tips in recent years. A schematic overview is displayed in Fig. 2.

(a) The basic probe is a sharpened glass tip, coated with metal, leaving an aperture at the apex. By pulling, etching and ion milling of glass rods or optical fibres, a tip radius as small as 10 nm can be fabricated. The aperture is formed by directional evaporation (2) or by subsequent cold deformation of the metal (3). The resulting aperture size ϕ is a combination of glass tip radius and penetration depth of the metal (e.g. 6.5 nm for aluminium), ϕ 20 nm being a practical lower limit. The efficiency of this probe type is low because: (1) the power of a light beam focused onto the aperture should be limited to 10-100 mW in order not to damage the metal coating. (2) The fraction of the focus that is illuminating the aperture is in the order of $(\phi/\lambda)^2$ due to the diffraction limit and a large fraction is reflected due to the cut-off size of the ultimate tip. (3) The fraction of the light on the aperture that propagates into the far field is proportional to $(\phi/\lambda)^4$ for an aperture ($\phi \ll \lambda$) surrounded by a perfect conductor. Consequently the total efficiency is proportional to $(\phi/\lambda)^6$ Typically for ϕ 50 nm about 10 nW light power extends into the far field. At the ultimate size of 20 nm, scanning a semi-transparent sample, generally less than 1 pW reaches the detector. The outer diameter of the probe at the apex is about 300 nm which limits the application to samples with gentle surface roughness. Betzig (2) has improved these probes by pulling adiabatically tapered single mode fibres which enable it to illuminate the aperture with a higher efficiency. With these probes 12 nm lateral resolution and polarisation contrast has been demonstrated.

(b) Micro-pipettes are an interesting alternative to the sharpened glass tips. The pipettes are pulled to an inner diameter of about 50 nm and subsequently coated with a suitable metal. The outer pipette diameter defines the light guide which has no cut-off size for the light propagating towards the aperture. Best results with a lateral resolution of about 50 nm have been obtained by Betzig (4) using these tips as detection probe, in the so-called "collection mode".

(c) The possibilities of the micro pipettes have been advantageously exploited by Lieberman (5) by growing dye crystals in the pipette core. Excitation of these nanometre size crystals produces excitons that undergo a radiative decay which is not limited by the cut-off criterion of propagation of light waves in the tip. Due to the non-evanescent character of the fluorescence the brightness of this miniature fluorescence light source is relatively high. A lateral resolution of 20-30 nm has been obtained.

(d) A sharp dielectric tip can be used as a probe for leaky waves. In this case the evanescent field has to be generated at the sample surface itself, which is generally accomplished by total internal reflection. The evanescent field is frustrated by the dielectric probe and converted into a propagating wave. Due to similarities with the STM this type of microscopy is often referred to as Photon Scanning Tunneling Microscopy (PSTM). This alternative probe is rather promising as it circumvents the problem of aperture fabrication and because the coupling is efficient, in principle up to 100% of the probed area. A lateral resolution of 30-100 nm is observed, determined by the sharpness of the tip, the tip-sample distance and by the evanescent field gradient. A disadvantage is its sensitivity for radiatively scattered waves. Near field microscopes based on this principle of localised frustrated total internal reflection have been realised by Ferrell (6), Courjon (7) and our group (8). A commercial version has recently been introduced (9). Operation of this probe in reflection has been shown by Courjon (10).

(e) Recently Fischer (11) has presented the concept and fabrication of an optical coaxial line, i.e. an optical fibre with a metal core, which has the advantage that its size can be reduced to typically 50 nm without limitation of wave propagation by a cut-off criterion. This type of probe is highly promising in view of its expected efficiency; however its merits in scanning microscopy have yet to be demonstrated.

The properties of the different probes described above have mostly been verified on suitable test samples. Initial applications towards imaging of bacteria and optical waveguides have been presented by Ferrell (6). Spectral analysis of near field luminescence has been reported by Paesler (12).

Evanescent field optical microscopy

Principle

We present recent advances with our evanescent field optical microscope (8). In this set-up the optical interaction between a dielectric probe tip (of type d) and a dielectric sample in the proximity is detected. The system is excited by an evanescent field which is generated by total internal reflection (TIR) within a substrate glass. The sample is placed on the glass surface, where the topographic and dielectric properties of the sample cause a modulation in the near field, consisting of both evanescent and homogeneous waves. The dielectric tip is approached towards the sample until within the evanescent field which causes frustrated TIR. The fraction of the evanescent field which is converted into a propagating wave is detected together with the contribution of other possible radiative waves over the surface. The tip is scanned over the sample surface either at a constant height, resulting in an image presenting the optical signal variation, or in closed loop ("optical tunneling"), resulting in an image representing topography and variation in dielectric constant.

Equipment used

The dielectric probe tips are fabricated by chemically etching a single mode fibre, yielding typically 20° apex and 100 nm radius. The evanescent field is generated by total internal reflection of a 8 mW HeNe laser beam (λ=632.8 nm) in a glass substrate (BK7, Schott). Samples are placed on the glass substrate together with an immersion liquid. The fraction of the laser

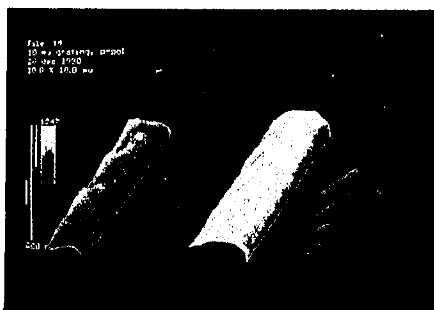

Fig. 6: 18.8×18.8 μm image in closed loop of a 10 μm period photoresist grating with steps 3.6 μm wide and 1.5 μm high with p-polarised (upper) and s-polarised (lower) laser beams.

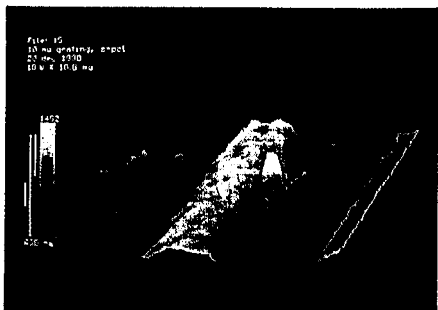

power coupled into the optical probe is typically 10^{-7}, mainly determined by the ratio between the probe tip area and the illuminated sample surface area. This optical power (0.1–1 nW) is detected with a photo multiplier tube (Hamamatsu R647-01). An image is obtained very similar to the STM by manipulating the optical probe tip with nanometer precision in lateral and vertical directions over the sample surface by means of a piezo-electric scanner (Microblock from Photon Control or piezo tube from Staveley Sensors Inc). A standard personal computer with data-acquisition cards is used for scan pattern generation, data collection and image display.

Results

Fig. 3 shows images of a silicon-nitride grating as obtained with two different tips. The grating has been fabricated by lithographic etching, using a 1 μm period mask, of a Si_3N_4 layer obtained by pressure enhanced chemical vapour deposition. Both figures 3a and 3b display imagess of a 3×3 μm area with steps 500 nm wide and 350 nm high, illuminated by TIR with a s-polarised beam and scanned in closed loop. Both images are plotted in 3D perspective and display the topographic structure associated to a surface of constant optical coupling without further filtering or smoothing of the data. In Fig. 3a the apparent image is a combination of grating topography and tip shape. Although the actual grating is flat on the top, as verified with an AFM, the top face of the grating steps display a smooth modulation pattern with a period of about the wavelength. This modulation reflects the presence of interfering scattered waves over the grating. In Fig. 3b the tip is much sharper with a small cone angle which enables it to follow the grating contour with an average edge width of 30 nm. This tip couples to the bottom of the trenches of the grating where topographic structure is resolved.

An image of latex spheres is shown in Fig. 4. The sample was prepared by evaporation of a suspension of ϕ 951 nm latex spheres in water and methanol. The surface was scanned in closed loop over 18.8×18.8 μm area. The spheres can be clearly distinguished and the detected peak height is 1.4 μm above the surface. To each sphere a ridge pattern is associated with a maximum height of about 90 nm. The direction of the ridges is determined by the direction of the incident laser beam, propagating from left to right in Fig. 4. They are not related to topographic features but display the response of the feedback system to interference phenomena.

The interference pattern is more prominent in Fig. 5 which displays the image of a single ϕ 91nm latex sphere, adsorbed to the substrate surface and scanned at constant height. The s-polarised laser beam is propagating from right to left. The image has been differentiated in the horizontal line scan direction in order to enhance the fringe pattern surrounding the sphere. The pattern displays the modulation in field intensity caused by interference between the field scattered by the sphere and the incident plane wave. The image is a kind of scanned hologram as it contains both amplitude and phase of the near field distribution of the sphere. The image cannot be recorded with any far field technique. The fringe period is about 300 nm ($\sim\lambda_2$) for scattering waves in the direction of the incident wave and increases towards the outgoing wave. The ϕ 91 nm latex sphere itself appears overexposed because its field intensity is more than two orders of magnitude larger than than of the surrounding fields and out of the range of the displayed colour scale.

Figure 6 shows images of a 10 μm period photoresist grating structure, with steps 3.6 μm wide and 1.5 μm high, for p- (Fig. 6a) and s-polarisation (Fig. 6b), both scanned with the same tip in closed loop. The plane of incidence is parallel to the grating lines. The p-polarisation image displays a rather rectangular grating with steps 4.3 μm wide and 1.5 μm high. The s-polarisation image only vaguely reveals the grating with 0.9 μm step height but shows more fine structure, which is a combination of topography and field distribution. The local peak in Fig. 6b represents, in our opinion, a field enhancement due to contamination or a tip touch. Comparison shows that s-polarised excitation tends to couple light in the lateral direction resulting in both wider and lower steps, whereas p-polarisation couples preferentially in the vertical direction.

Conclusion

Our results clearly demonstrate the capacity of the evanescent field optical microscope to circumvent the diffraction limit and obtain sub-wavelength resolution. The lateral resolution of ~30 nm is determined not only by the sharpness of the probe tip but also by the exponential decay of the evanescent field itself, which can be controlled by choosing angle of incidence, working distance and wavelength. The highest resolution is observed in closed loop. The vertical resolution of 0.1 nm is mainly limited by electronics and piezo hysteresis.

The apparent images depend on polarisation, as the direction of the exciting field affects both the optical coupling efficiency and resolution. The optical coupling occurs preferentially in the direction parallel to the exciting electric field. As a result p-polarisation images correspond well to the vertical topographic structure, whereas s-polarisation couples less efficient and is more suitable for lateral structures.

Near field diffraction patterns are observed with high lateral resolution by interference between evanescent and propagating waves. These patterns enable detailed analysis of amplitude and phase of near field Fresnel diffraction. On the other hand the scattered light affects the feedback action and the interference may dominate any topographic fine structure. Therefore, although the classical diffraction limit is surpassed in resolution, still the presence of radiative waves could pose a problem in the application of near field optical microscopy.

Perspective

Near field optical microscopy is presently moving from development into the application stage. Lateral resolution is approaching 10 nm. The feasibility of polarisation contrast and spectroscopic analysis has been proven. The technique is unique among the scanning probe microscopies as it probes dielectric properties; as such it is a useful extension to STM and AFM when applied to optical surfaces (thin films, photo lithographic process, etc.) biological surfaces (membranes, chromosomes, lipids, proteins) and chemical surfaces (polymers, Langmuir Blodgett films). The spectroscopic potential can be applied to surfaces labelled by fluorophores or immunogold techniques. Alternatively the technique might enable high resolution pattern generation in photoresist layers. Still it should be recognised that any future application of near field optical microscopy depends completely on the development of reliable and efficient tips.

References

1. Fischer, U.Ch., Resolution and contrast generation in scanning near field optical microscopy. *Scanning Tenneling Microscopy and Related Methods* (ed. by R.J. Behm), pp. 475-496. Kluwer Academic Publishers, The Netherlands, 1990.

2. Betzig, E., Trautman, J.K., Harris, T.D., Weiner, J.S. and Kostelak, R.L. Breaking the Diffraction Barrier: Optical Microscopy on a Nanometric Scale. *Science*, **251**, 1468-1470, 1991.

3. Dürig, U., Pohl, D.W. and Rohner, F. Near-field optical-scanning microscopy. *J. Appl. Phys.*, **59**, 3318-3327, 1986.

4. Betzig, E., Isaacson, M. and Lewis, A. Collection mode near-field optical microscopy. *Appl. Phys. Lett.*, **51**, 2088-2090, 1987.

5. Lieberman, K., Harush, S., Lewis, A. and Kopelman, R. A Light Source Smaller than the Optical Wavelength. *Science*, **247**, 59-61, 1990.

6. Ferrell, T.L., Goundonnet, J.P., Reddick, R.C., Sharp, S.L. and Warmack, R.J. The photon scanning tunneling microscope, *J. Vac. Sci. Technol.*, **B9**, 525-529, 1991.

7. Courjon, D., Scanning Tunneling Optical Microscopy. *Scanning Tunneling Microscopy and Related Methods* (ed. by R.J. Behm), pp. 497-505, 1990. Kluwer Academic Publishers, The Netherlands.

8. van Hulst, N.F., de Boer, N.P. and Bölger, B. An Evanescent Field Optical Microscope. *J. Microscopy*, **163**, 117-130, 1991; van Hulst, N.F., Evanescent Field Optical Microscopy, *Microscopy & Analysis*, **11**, 7, 1991.

9. SPIRAL Recherche & Developpment, Dijon, France.

10. Courjon, D., Vigoureux, J.-M., Spajer, M., Sarayeddine, K. and Leblanc, S. External and internal reflection near field microscopy: experiments and results, *Appl. Opt.* **29**, 3734-3740, 1990.

11. Fischer, U.Ch., The wire probe for Scanning Near Field Optical Microscopy (SNOM), presented at STM '91, Intelarken, 1991.

12. Paesler, M.A., Moyer, P.J., Jahncke, C.J., Johnson, C.E., Reddick, R.C., Warmack, R.J. and Ferrell, T.L. Analytical Photon Scanning Tunneling Microscopy, *Phys. Rev.* **B42**, 6750-6753, 1990.

Authors address: Niko F van Hulst & Frank B Segerink, Opto-electronics, Applied Physics, University of Twente, PO Box 217, 7500 AE Enschede, The Netherlands.